Nonlinear evolution of disturbances in higher time-derivative theories

Andreas Fring [ID],[a] **Takano Taira** [ID][b] **and Bethan Turner**[a]

[a]*Department of Mathematics, City, University of London,*
Northampton Square, London EC1V 0HB, U.K.

[b]*Research Fellow of Japan Society for Promotion of Science, Institute of Industrial Science,*
The University of Tokyo,
5-1-5 Kashiwanoha, Kashiwa 277-8574, Japan

E-mail: a.fring@city.ac.uk, taira904@iis.u-tokyo.ac.jp,
bethan.turner.2@city.ac.uk

ABSTRACT: We investigate the evolution of localized initial value profiles when propagated in integrable versions of higher time-derivative theories. In contrast to the standard cases in nonlinear integrable systems, where these profiles evolve into a specific number of N-soliton solutions as dictated by the conservation laws, in the higher time-derivative theories the theoretical prediction is that the initial profiles can settle into either two-soliton solutions or into any number of N-soliton solutions. In the latter case this implies that the solutions exhibit oscillations that spread in time but remain finite. We confirm these analytical predictions by explicitly solving the associated Cauchy problem numerically with multiple initial profiles for various higher time-derivative versions of integrable modified Korteweg-de Vries equations. In the case with the theoretical possibility of a decay into two-soliton solutions, the emergence of underlying singularities may prevent the profiles from fully developing or may be accompanied by oscillatory, chargeless standing waves at the origin.

Contents

1 Introduction

The emergence of stable soliton solutions from the evolution of generic initial profiles in continuous versions [1] of the seminal Fermi-Pasta-Ulam-Tsingou models [2, 3] is one of the archetypical effects in classical nonlinear integrable field theories. The integrability of the models ensures that the system evolves into some of the N-soliton solutions of the underlying nonlinear integrable equation when $N > 1$. Following [4, 5] one can employ the conservation laws of the model and predict how many solitons will emerge together with their amplitudes. Here, our main purpose is to investigate the analogue of this phenomenon in a set of integrable higher time-derivative theories (HTDT).

Despite the fact that HTDT unavoidably contain singularities in their classical solutions and lead to inconsistent quantum versions, they have kept being of interest because at the same time they also posses a number of very attractive features, such as being renormalizable [6–11]. Several proposals have been made to resolve the issues of non-normalisable states and/or the unboundedness of their spectra in the quantum version of HTDT [12–16]. HTDT have been applied in a variety of areas in physics, such as in attempts to quantize gravity [17], in applications to cosmology [18–21], finite temperature physics [22], black hole solutions [23], BRST quantisation [24, 25], in a massless particle descriptions of bosons and fermions [26, 27] and in supersymmetric theories [28, 29]. Classical and quantum stability properties of HTDT were investigated in [30–35].

There are of course many different versions of HTDT, [6-35]. Here we will follow a recent suggestion [36] and focus our investigations on a particular class of models that are obtained from exchanging space and time in Hamiltonian and higher charge systems of modified Korteweg-de Vries type. For the specific example such an idea was previously

pursued in [37]. While in general the original versions of higher charge theories are still of interest in their own right [38, 39], we continue here our investigation from [40] on HTDT by concentrating on the study of soliton solutions in these systems. Here we focus in particular on the previously not investigated aspect of how an initial profile evolves into an analytical soliton solution as dictated by integrability. The result will shed new light on the nature of the instabilities inevitably present in HTDTs.

Our manuscript is organised as follows: In section 2 we recall the standard argument of how to predict the amplitudes of the emerging solitons for a given initial value profile and discuss how this reasoning needs to be modified for HTDT. In section 3 we carry out a detailed analytical and numerical analysis of the emergent solitons in the standard KdV system, some of its higher charge Hamiltonian systems, the integrable modified KdV system and their nonintegrable modified versions. In section 4 we carry out the adequately modified analysis for the HTDT of the systems considered in section 3. Our conclusions are stated in section 5.

2 Emergent solitons from initial value disturbances

We briefly recall from [4] the standard argument of how the conservation laws of integrable systems can be used to predict the amplitudes of the emergent solitons from an initial value profile that is evolved with an integrable nonlinear equation and elaborate on how it needs to be modified for HTDT. In general, we are considering here the following Cauchy initial value problem

$$u_t = F(u, u_x, \ldots, u_{nx}), \qquad u(x, t=0) = f(x), \quad \lim_{|x| \to \infty} u(x,t), \ldots, u_{(n-1)x}(x,t) = 0, \quad (2.1)$$

where the function F might be nonlinear in the fields u and its partial x-derivatives up to order n and the function $f(x)$ characterises the initial value profile.

The system is assumed to be integrable so that one can exploit infinitely many conservation laws of the form

$$\frac{\partial Q_\ell(x,t)}{\partial t} + \frac{\partial \chi_\ell(x,t)}{\partial x} = 0, \qquad \ell \in \mathbb{N}, \quad (2.2)$$

relating the charge densities Q_ℓ to the flux densities χ_ℓ. Then $\mathcal{Q}_\ell(t) = \int_{-\infty}^{\infty} Q_\ell(x,t)dx$ is conserved in time, i.e. $d\mathcal{Q}/dt = 0$ for $\lim_{|x| \to \infty} \chi_\ell(x,t) = 0$, where the latter is ensured by our asymptotic conditions in (2.1). It is well-known that any N-soliton solution behaves asymptotically in time as the sum of N one-soliton solutions. Therefore, the corresponding charges $\mathcal{Q}_\ell^{(N)}(a_1, \ldots, a_N)$, depending on some parameters a_i, such as for instance the amplitudes, is the sum of the asymptotically acquired one-soliton contributions, i.e., $\mathcal{Q}_\ell^{(N)} = \sum_{i=1}^{N} \mathcal{Q}_\ell^{(1)}(a_i)$. Assuming that the initial profile breaks up into an N-soliton then implies that for each charge the entire initial profile charge $\mathcal{Q}_\ell^{(I)}$ is converted into the sum of the one-soliton contributions to that charge, i.e.,

$$\mathcal{Q}_\ell^{(I)} = \int_{-\infty}^{\infty} Q_\ell \left[u(x,0) \right] dx = \sum_{i=1}^{N} \mathcal{Q}_\ell^{(1)}(a_i). \quad (2.3)$$

At this point it is still not determined into how many solitons N the initial profile will evolve. However, each of the equations in (2.3) provides a constraint, which can be used to answer

this question in concrete models. Moreover, one can solve the system of equations (2.3) for the amplitudes a_i to predict them in an approximate fashion. In [4] only combination of the lowest charges were taken into account to make theoretical predictions. However, one should stress that all possibilities need to be respected, which makes this system of equations highly overdetermined. Here we refine the analysis of [4] by including more combinations into the analysis. Thus, our approach leads to more detailed predictions and crucially, especially for HTDT, also predicts when a break up into multi-soliton solution is prohibited.

In HTDT the Cauchy problem (2.1) must be changed into

$$0 = F(u, u_x, \ldots, u_{nx}, u_t, \ldots, u_{mt}), \qquad u(x, 0) = f_1(x), \ldots, u_{(m-1)t}(x, 0) = f_{(m-1)}(x), \quad (2.4)$$

together with adequate boundary conditions. All m functions f_i are independent. Following [40–42] we assume here in the first instance that the HTDT is obtained from (2.1) by exchanging time and space, i.e. $x \leftrightarrow t$. This approach allows us to use the conservation laws (2.3) with $Q_\ell(x, t) \leftrightarrow \chi_\ell(t, x)$ and make similar prediction for the number of solitons and their amplitudes in these theories into which the initial profiles $f_1, \ldots f_m$ evolve. The interesting aspect to be investigated here is how the different types of singularities, that are inevitable present in a HTDT, manifest themselves in this break up process.

3 Emergent solitons in modified Korteweg-de Vries systems

We start our investigation with the series of the modified KdV system in the form

$$u_t + n(n-1)u^{n-2}u_x + u_{xxx} = 0, \qquad n \in \mathbb{N}. \quad (3.1)$$

Rescaling equation (3.1) by

$$x \to \frac{\sigma^2 \lambda_n^{3-2n}}{(n-1)^2 n^2} x, \quad t \to \lambda_n t, \quad u \to \lambda_n u, \quad \lambda_n := \left[\frac{(n-1)^3 n^3}{\sigma^2} \right]^{\frac{1}{4-3n}}, \quad (3.2)$$

we obtain

$$u_t + u^{n-2}u_x + \frac{1}{\sigma^2}u_{xxx} = 0. \quad (3.3)$$

Next we solve the Cauchy problem for equation (3.3) with initial value profile $u(x, t = 0) = f(x)$ and vanishing asymptotic values $\lim_{|x| \to \infty} u(x, t), u_t(x, t), u_{tt}(x, t) = 0$. In accordance with the similarity principle the parameter σ, that was introduced through the scaling (3.2), is known to separate regions of different characteristic behaviour [4]. Letting the initial profile evolve by means of (3.3), the integrability of the models for $n = 3, 4$ ensures that the profile will eventually settle into a multi-soliton solution and hence for large times into a number of one-soliton solutions. For the nonintegrable systems with $n > 4$ no solitons are expected to emerge.

3.1 Emergent solitons in the Korteweg-de Vries system

The first case we consider is to revisit the standard KdV-equation corresponding to the equation of motion (3.1) with $n = 3$. We recall from [43–45] the charge and flux densities of

the first four conserved quantities, which when appropriately scaled become

$$Q_1 = u, \qquad\qquad\qquad \chi_1 = \frac{1}{2}u^2 + \frac{1}{\sigma^2}u_{xx}, \qquad\qquad (3.4)$$

$$Q_2 = \frac{1}{2}u^2, \qquad\qquad\qquad \chi_2 = \frac{1}{3}u^3 + \frac{1}{2\sigma^2}\left(2uu_{xx} - u_{xx}^2\right),$$

$$Q_3 = \frac{1}{3}u^3 - \frac{1}{\sigma^2}u_x^2, \qquad\qquad \chi_3 = \frac{1}{4}u^4 + \frac{1}{\sigma^2}\left(u^2 u_{xx} + 2uu_x\right) + \frac{1}{\sigma^4}u_{xx}^2,$$

$$Q_4 = \frac{1}{4}u^4 - \frac{3}{\sigma^2}uu_x^2 + \frac{9}{5\sigma^4}u_{xx}^2,$$

$$\chi_4 = \frac{1}{5}u^5 + \frac{1}{\sigma^2}\left(u^3 u_{xx} - \frac{9}{2}u^2 u_x^2\right) + \frac{3}{\sigma^4}\left(u_x^2 u_{xx} - 2uu_x u_{xxx} + \frac{8uu_{xx}^2}{5}\right)$$

$$- \frac{9}{5\sigma^6}\left(u_{xxx}^2 - 2u_{xx}u_{xxxx}\right).$$

For the one-soliton solution of (3.3)

$$u(x,t) = a\operatorname{sech}^2\left[\frac{\sigma}{\sigma_s}\sqrt{a}\left(x - \frac{a}{3}t\right)\right], \qquad\qquad (3.5)$$

with nonlinearity index $\sigma_s = \sqrt{12}$, we compute with (3.4) the conserved charges

$$\mathcal{Q}_1 = \frac{2\sigma_s\sqrt{a}}{\sigma}, \qquad \mathcal{Q}_2 = \frac{2\sigma_s a^{3/2}}{3\sigma}, \qquad \mathcal{Q}_3 = \frac{4\sigma_s a^{5/2}}{15\sigma}, \qquad \mathcal{Q}_4 = \frac{4\sigma_s a^{7/2}}{35\sigma}. \qquad (3.6)$$

Thus, if the initial profile would be converted entirely into a one-soliton solution, relation (2.3) implies that $\mathcal{Q}_\ell = \mathcal{Q}_\ell^{(I)}$. In principle, these relations could be used to predict the amplitude of the emerging soliton. However, when solved for the amplitudes as functions of σ these equations lead to vastly mismatching solutions for different values of ℓ and hence the solution is not unique, see the yellow region in figure 1 for some examples. The marked amplitudes of some solitary waves obtained from the numerical solutions are very crudely identified, as we have ignored the typical oscillatory tail that spreads to negative infinity as time evolves. This means the various constraints imposed by the integrability of the system prevent a full conversion of the initial profile into a one-soliton, so that the region $\sigma < \sigma_c$ in which no multi-soliton can form, is referred to as a "nonsoliton" region [4]. In this region the initial disturbance decays into an oscillating wave that spreads throughout space.

Assuming instead that the initial profile evolves into a two-soliton with amplitudes a_1 and a_2, relation (2.3) yields the two constraining equations from the first two equation with $\ell = 1$ and $\ell = 2$

$$\sqrt{a_1} + \sqrt{a_2} = \frac{\sigma}{2\sigma_s}\mathcal{Q}_1^{(I)} =: I_1, \qquad \text{and} \qquad a_1^{3/2} + a_2^{3/2} = \frac{3\sigma}{2\sigma_s}\mathcal{Q}_2^{(I)} =: I_2, \qquad (3.7)$$

which are easily solved to

$$a_{1/2} = \left(\frac{I_1}{2} \pm \frac{\sqrt{4I_1 I_2 - I_1^4}}{2\sqrt{3}I_1}\right)^2. \qquad\qquad (3.8)$$

Demanding the amplitudes to be real and its square roots to be positive, as assumed in (3.7), gives the following interval for σ in which the initial profile may consistently evolves into
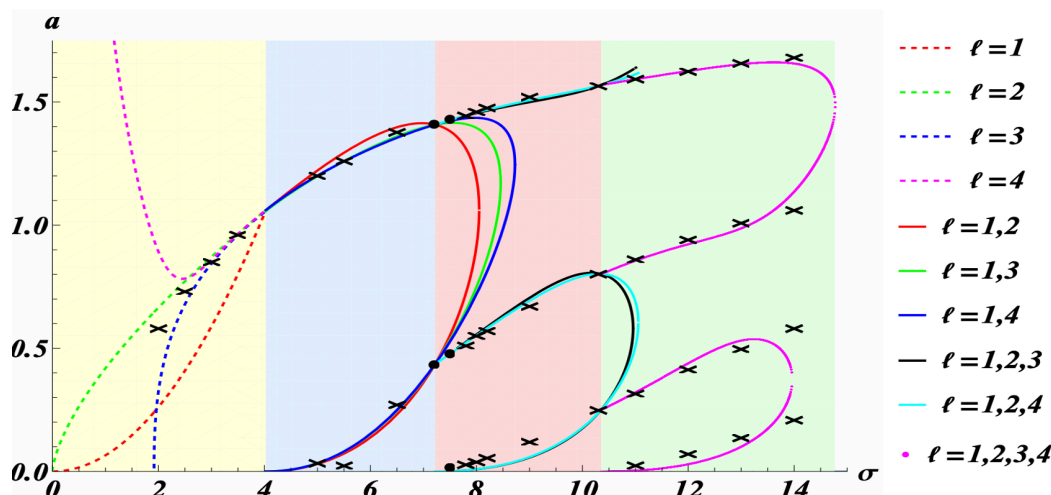
Figure 1. Domains of N-soliton states emerging from an initial Gaussian profile in the KdV system together with their predicted amplitudes. The nonsoliton, two-soliton, three-soliton and four-soliton regions are shaded in yellow, blue, red and green, respectively. The black crosses and dots represent the values of the amplitudes from the actual numerical solutions of the Cauchy problem for specific values of σ. For the values of the black dots we show the explicit solutions in figure 2.

two-soliton solutions

$$\sigma_c < \sigma < 2\sigma_c, \qquad \sigma_c = 12\sqrt{\mathcal{Q}_2^{(I)}/\left(\mathcal{Q}_1^{(I)}\right)^3}. \tag{3.9}$$

For a Gaussian initial profile $f(x) = e^{-x^2}$ we obtain from (2.3)

$$\mathcal{Q}_1^{(I)} = \sqrt{\pi}, \quad \mathcal{Q}_2^{(I)} = \sqrt{\frac{\pi}{2^3}}, \quad \mathcal{Q}_3^{(I)} = \sqrt{\frac{\pi}{3^3}} - \frac{1}{\sigma^2}\sqrt{\frac{\pi}{2}}, \quad \mathcal{Q}_4^{(I)} = \frac{\sqrt{\pi}}{8} - \frac{2}{\sigma^2}\sqrt{\frac{\pi}{3}} + \frac{1}{\sigma^4}\frac{27}{5}\sqrt{\frac{\pi}{2}}. \tag{3.10}$$

This information is sufficient to predict the amplitudes in the different N-soliton regions.

The bounds for the two-soliton region (3.9) are then characterised by $\sigma_c = 6 \times 2^{1/4}/\sqrt{\pi} \approx 4.026$, which is in agreement with [4]. However, here we refine this analysis and consider also solutions from combining conservation laws for different values of ℓ. In figure 1 we have included for a variety of combinations the numerically obtained predicted amplitudes together with the actual numerical solutions of the initial value problem.

For the two-soliton case we observe that, unlike as in the nonsoliton region, there are regions for which the predicted amplitudes from different combinations roughly coincide. For $\sigma_c < \sigma \lessapprox 7.22$ the two one-soliton solutions are formed with small deviations from the anticipated amplitudes because each combination of the conservation laws leads to slightly different predictions. For $\sigma \approx 7.22$ the agreement is extremely good, since all the predicted amplitudes almost exactly coincide, the system is left with no ambiguities into which solution to settle, see figure 2 panel (a).

However, in the region $\sigma \gtrsim 7.22$ the predictions start to differ more significantly. Moreover, beyond that value even three-soliton solution may occur, hence the "three-soliton region" is partially encroaching into the "two-soliton region" that was predicted in [4]. In figure 1
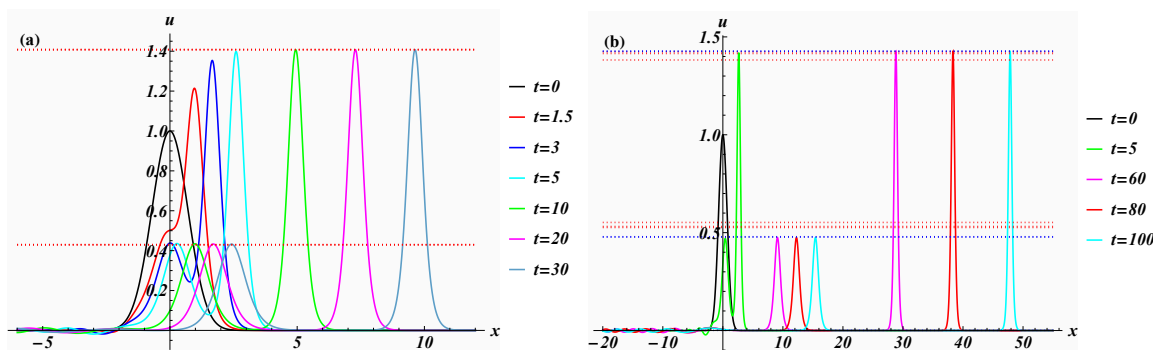
Figure 2. Evolution of an initial Gaussian profile into a two-soliton solution panel (a) and three-soliton solution panel (b) as time evolves for the KdV system for $\sigma = 7.2$ and $\sigma = 7.5$, respectively. The predicted two and three-soliton amplitudes are depicted as dotted red and blue lines, respectively.

we have also included some solutions for these cases computed numerically from solving the three equations

$$\sum_{i=1}^{3} \sqrt{a_i} = \frac{\sigma}{2\sigma_s} \mathcal{Q}_1^{(I)}, \qquad \sum_{i=1}^{3} a_i^{3/2} = \frac{3\sigma}{2\sigma_s} \mathcal{Q}_2^{(I)}, \qquad \sum_{i=1}^{3} a_i^{5/2} = \frac{15\sigma}{4\sigma_s} \mathcal{Q}_3^{(I)}. \tag{3.11}$$

We see in figure 1 that the predicted amplitudes from combining different combinations of the conservation laws matches quite well the actual numerical solution. We also note in panel (b) of figure 2 that the acquired values in the "two-soliton region" are in fact those predicted for the three-soliton with one of the amplitudes being very small so that the solutions only appears to be a two-soliton. We have also included the predictions of the four-soliton solutions which start to emerge at around $\sigma \approx 10.355$ where all the three-soliton predictions and the largest amplitudes of the four-soliton prediction coincide.

The observed features suggest more generally that *an initial profile will always break up into the maximal number of one-solitons that is allowed by the conservation laws (2.3)*.

3.2 Emergent solitons in higher charge KdV Hamiltonian systems

Next we interpret the higher KdV charge $\mathcal{Q}_4$ as a Hamiltonian. In order to derive Hamilton's equation of motion we need to identify the canonical fields. Here we may achieve this by a direct extrapolation from the standard Hamiltonian system [46], for a more general treatment see [40]. Multiplying this charge by $-1/3$, introducing the canonical momentum field $\pi = \psi_x/2$ by adding zero to it and replacing $u \to \psi_x$, we obtain the higher charge Hamiltonian density

$$\mathcal{H}_4 = \pi \psi_t - \frac{1}{2} \psi_t \psi_x - \frac{1}{12} \psi_x^4 + \frac{1}{\sigma^2} \psi_x \psi_{xx}^2 - \frac{3}{5\sigma^4} \psi_{xxx}^2. \tag{3.12}$$

The corresponding Hamilton's equations resulting from this Hamiltonian are

$$\psi_t = \frac{\delta \mathcal{H}_4}{\delta \pi} = \frac{\partial \mathcal{H}_4}{\partial \pi} = \psi_t, \tag{3.13}$$

$$\pi_t = -\frac{\delta \mathcal{H}_4}{\delta \phi} = -\left[\frac{\partial \mathcal{H}_4}{\partial \psi} - \partial_x \left(\frac{\partial \mathcal{H}_4}{\partial \psi_x} \right) + \partial_x^2 \left(\frac{\partial \mathcal{H}_4}{\partial \psi_{xx}} \right) - \partial_x^3 \left(\frac{\partial \mathcal{H}_4}{\partial \psi_{xxx}} \right) \right] \tag{3.14}$$

$$= -\frac{1}{2} \psi_{xt} - \frac{1}{3} (\psi_x^3)_x + \frac{1}{\sigma^2} (\psi_{xx}^2)_x - \frac{2}{\sigma^2} (\psi_x \psi_{xx})_{xx} - \frac{6}{5\sigma^4} (\psi_{xxx})_{xxx}.$$

In terms of the standard field u the equation of motion reads

$$u_t + u^2 u_x + \frac{2}{\sigma^2}\left[(u_x^2)_x + u u_{xxx}\right] + \frac{5}{6\sigma^4}u_{5x} = 0. \tag{3.15}$$

We find a one-soliton solution for (3.15)

$$u(x,t) = a\,\mathrm{sech}^2\left[\frac{\sigma}{\sigma_s}\sqrt{a}\left(x - \frac{2a^2}{15}t\right)\right]. \tag{3.16}$$

The charges obtained from integrating the densities (3.4) are also conserved, subject to the equation of motion (3.15). The fluxes will of course change. We report the first three expressions

$$\chi_1 = \frac{u^3}{3} + \frac{1}{\sigma^2}\left(u_x^2 + 2u u_{xx}\right) + \frac{6}{5\sigma^4}u_{4x}, \tag{3.17}$$

$$\chi_2 = \frac{u^4}{4} + \frac{2}{\sigma^2}u^2 u_{xx} + \frac{3}{5\sigma^4}\left(2u u_{4x} - 2u_x u_{xxx} + u_{xx}^2\right), \tag{3.18}$$

$$\chi_3 = \frac{u^5}{5} + \frac{2}{\sigma^2}u^2\left(u u_{xx} - u_x^2\right) + \frac{2}{5\sigma^4}\left[u\left(3u u_{4x} + 8u_{xx}^2\right) - 14u_x^2 u_{xx} - 16u u_x u_{xxx}\right] \tag{3.19}$$
$$+ \frac{6}{5\sigma^6}\left(2u_{4x}u_{xx} - 2u_x u_{5x} - u_{xxx}^2\right).$$

Since the static part of the two one-soliton solutions (3.5) and (3.16) coincide, and also the general expression for the corresponding charges are identical, the predictions for the amplitudes and the number of one-solitons to emerge are the same. The only difference between (3.5) and (3.16) are the soliton speeds $v_1 = a/3$ and $v_2 = 2a^2/15$, respectively. Since $v_2 < v_1$ for $0 < a < 5/2$ and the upper bound for any of the acquired one-soliton amplitudes is 2, see [47], the solitons in the higher charge Hamiltonian system will always be identical in height but slower than those in the original KdV equation. We have verified this numerically.

3.3 Emergent solitons in the modified Korteweg-de Vries equation

Next we consider modified KdV-equation corresponding to (3.1) with $n = 4$, which in standard terminology is the original modified KdV equation. The associated charge and flux densities of the first five conserved quantities can be found in [43–45], and when scaled appropriately read

$$Q_1 = \frac{1}{2}u^2, \qquad \chi_1 = \frac{1}{4}u^4 + \frac{1}{\sigma^2}\left(u u_{xx} - \frac{1}{2}u_x^2\right), \tag{3.20}$$

$$Q_2 = \frac{1}{4}u^4 - \frac{3}{2\sigma^2}u_x^2, \qquad \chi_2 = \frac{1}{6}u^6 + \frac{1}{\sigma^2}\left(u^3 u_{xx} - 3u^2 u_x^2\right) + \frac{3}{\sigma^4}\left(\frac{1}{2}u_{xx}^2 - u_x u_{xxx}\right),$$

$$Q_3 = \frac{1}{6}u^6 - \frac{5}{\sigma^2}u^2 u_x^2 + \frac{3}{\sigma^4}u_{xx}^2,$$

$$\chi_3 = \frac{1}{8}u^8 + \frac{1}{2\sigma^2}\left(2u^5 u_{xx} - 15u^4 u_x^2\right) + \frac{1}{2\sigma^4}\left[4u^2\left(4u_{xx}^2 - 5u_x u_{xxx}\right) + 20u u_x^2 u_{xx} + u_x^4\right]$$
$$+ \frac{1}{\sigma^6}\left(6u_{xx}u_{xxxx} - 4u_{xxx}^2\right),$$

$$Q_4 = \frac{u^8}{8} - \frac{21}{2\sigma^2}u^4 u_x^2 - \frac{63}{10\sigma^4}\left(u_x^4 - 2u^2 u_{xx}^2\right) - \frac{27}{5\sigma^6}u_{xxx}^2,$$

$$\chi_4 = \frac{1}{10}u^{10} + \frac{1}{\sigma^2}u^6\left(uu_{xx} - 14u_x^2\right) - \frac{21}{10\sigma^4}u^2\left(10u^2u_xu_{xxx} - 11u^2u_{xx}^2 - 20uu_x^2u_{xx} + 12u_x^4\right)$$

$$- \frac{9}{5\sigma^6}\left(10u^2u_{xxx}^2 - 14u^2u_{4x}u_{xx} + 28uu_xu_{xx}u_{xxx} + u_x^2u_{xx}^2 + 14u_x^3u_{xxx} - 2uu_{xx}^3\right)$$

$$+ \frac{27}{5\sigma^8}\left(u_{4x}^2 - 2u_{5x}u_{xxx}\right),$$

$$\mathcal{Q}_5 = \frac{1}{10}u^{10} - \frac{18}{\sigma^2}u^6u_x^2 + \frac{18}{5\sigma^4}u^2\left(9u^2u_{xx}^2 - 19u_x^4\right) + \frac{108}{35\sigma^6}\left(51u_x^2u_{xx}^2 + 20uu_{xx}^3 - 9u^2u_{xxx}^2\right)$$

$$+ \frac{324}{35\sigma^8}u_{4x}^2.$$

We will not report the flux χ_5 here as it is rather lengthy. For the one-soliton solution of (3.1) with $n = 4$

$$u(x,t) = a\,\mathrm{sech}\left[\frac{a\,\sigma}{\sqrt{6}}\left(x - \frac{a^2}{6}t\right)\right], \tag{3.21}$$

we compute the values of the conserved charges

$$\mathcal{Q}_1 = \frac{\sqrt{6}\,a}{\sigma}, \qquad \mathcal{Q}_2 = \frac{a^3}{\sqrt{6}\sigma}, \qquad \mathcal{Q}_3 = \frac{a^5}{5\sqrt{6}\sigma}, \quad \mathcal{Q}_4 = \frac{\sqrt{3}a^7}{70\sqrt{2}\sigma}, \quad \mathcal{Q}_5 = \frac{a^9}{105\sqrt{6}\sigma}, \tag{3.22}$$

and also the values the charges (2.3) acquire with the same Gaussian initial profile as previously

$$\mathcal{Q}_1^{(I)} = \frac{1}{2}\sqrt{\frac{\pi}{2}}, \qquad \mathcal{Q}_2^{(I)} = \frac{\sqrt{\pi}}{8} - \frac{3}{2\sigma^2}\sqrt{\frac{\pi}{2}}, \qquad \mathcal{Q}_3^{(I)} = \frac{1}{6}\sqrt{\frac{\pi}{6}} - \frac{5\sqrt{\pi}}{4\sigma^2} + \frac{9}{\sigma^4}\sqrt{\frac{\pi}{2}}, \tag{3.23}$$

$$\mathcal{Q}_4^{(I)} = \frac{1}{16}\sqrt{\frac{\pi}{2}} - \frac{7}{2\sigma^2}\sqrt{\frac{\pi}{6}} + \frac{1197\sqrt{\pi}}{80\sigma^4} - \frac{81}{\sigma^6}\sqrt{\frac{\pi}{2}}.$$

$$\mathcal{Q}_5^{(I)} = \frac{1}{10}\sqrt{\frac{\pi}{10}} - \frac{9}{4\sigma^2}\sqrt{\frac{\pi}{2}} + \frac{62\sqrt{6\pi}}{5\sigma^4} - \frac{15741\sqrt{\pi}}{70\sigma^6} + \frac{486\sqrt{2\pi}}{\sigma^8} \tag{3.24}$$

As explained in much detail in the previous sections, we use the charge conservation equation (2.3) for various combinations to determine the different soliton regions. Taking $\ell = 1, 2$ we compute the predicted two-soliton amplitudes to

$$a_\pm = \frac{\sqrt{3\pi}\sigma^2 \pm \sqrt{288\sqrt{2}\sigma^2 - \pi\sigma^4 - 3456}}{24\sigma}. \tag{3.25}$$

For $3.0213 \approx \left(24\sqrt{2}\left(6 - \sqrt{36 - 3\pi}\right)/\pi\right)^{1/2} \leq \sigma \leq \left(24\sqrt{2}\left(6 + \sqrt{36 + 3\pi}\right)/\pi\right)^{1/2} \approx 10.9781$ these amplitudes are real. We also compute the predicted three-soliton amplitudes by taking $\ell = 1, 2, 3$, which turn out to be real for $7.392064 \leq \sigma \leq 14.947399$. Thus compared to the prediction for the KdV equation we have a much larger overlap between the two and three-soliton region. A comparison with the actual numerical results from evolving the initial profile is presented in figure 3.

We observed that once a three-soliton is possible to occur, the numerical solutions do in fact settle into them. The same holds for the predicted four-soliton amplitude predictions, that are also included into figure 3, when compared to the three soliton predictions. This observation confirms the general statement made at the end of section 3.1, that an initial profile always breaks up into the maximal possible number of multi-solitons.
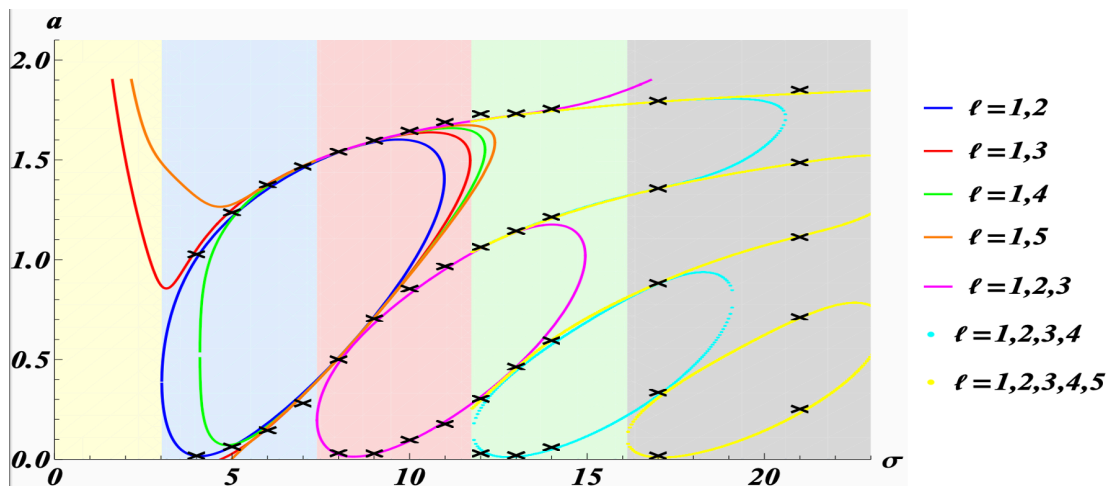
Figure 3. Domains of N-soliton states emerging from an initial Gaussian profile in the mKdV system together with their predicted amplitudes. Colour conventions are the same as in figure 1 with the addition of the five-soliton region in grey.
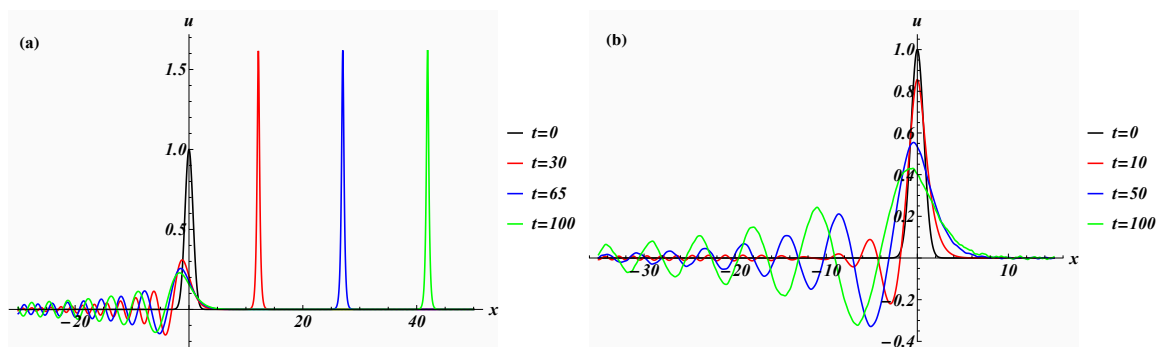
Figure 4. Evolution of an initial Gaussian profile in nonintegrable versions of the modified KdV equations with $n = 5$, $\sigma = 7$ and $n = 6$, $\sigma = 4$ in panel (a) and panel (b), respectively.

3.4 Solitary waves in the nonintegrable modified KdV equations

For completeness we also present here two examples for a nonintegrable version of (3.1), i.e. for $n > 4$. For these values the initial profile does not break up into a multi-soliton solution. However, the characteristic behaviour for $n = 5$ is different from the other cases as exemplified for two cases in figure 4. In the $n = 5$ case, panel (a), the solution behaves very much like the integrable cases in the nonsoliton region, i.e. the initial disturbance settles into a moving solitary wave, but also maintains an oscillatory tail for negative x. However, even for larger σ we did not observe any break up into multi-soliton solutions, which is of course a signature of the model not being integrable. In contrast, in the other cases the initial disturbance only transforms into an oscillatory tail that stretches more and more in space as time evolves. No solitary waves are emerging in these cases, see panel (b) for an example.

4 Emergent solitons in HTDT versions of modified KdV equations

Next we consider the rotated version of equation (3.3) with time and space exchanged

$$u_x + u^{n-2}u_t + \frac{1}{\sigma^2}u_{ttt} = 0, \tag{4.1}$$

and solve the rotated Cauchy problem (2.4) for this equation with initial value profile $u(x, t = 0) = f_1(x)$, $u_t(x, t = 0) = f_2(x)$, $u_{tt}(x, t = 0) = f_2(x)$, and vanishing asymptotic values $\lim_{|x|\to\infty} u(x, t) = 0$. Equivalently, we may of course also rotate (3.1) and change the scaling (3.2) appropriately to obtain (4.1).

4.1 Emergent solitons in the HTDT version of the KdV system

As mentioned in section 2, in the rotated case the conserved quantities are the same as in the original equation with $x \leftrightarrow t$ and $Q_\ell(x, t) \leftrightarrow \chi_\ell(t, x)$, i.e., the first charge and flux densities in the rotated case for $n = 3$ read

$$Q_1 = \frac{1}{2}u^2 + \frac{1}{\sigma^2}u_{tt}, \ \chi_1 = u, \quad Q_2 = \frac{1}{3}u^3 + \frac{1}{2\sigma^2}\left(2uu_{tt} - u_{tt}^2\right), \ \chi_2 = \frac{1}{2}u^2, \quad \text{etc.} \tag{4.2}$$

We find the following one-soliton solution to (4.1) for $n = 3$

$$u(x, t) = a\operatorname{sech}^2\left[\frac{\sigma}{\sigma_s}\frac{a^{3/2}}{3}\left(x - \frac{3}{a}t\right)\right]. \tag{4.3}$$

In general, the solutions for the rotated KdV system were found to be unstable [41, 42], in the sense that they develop singularities of different type, as was discussed in detail in [40] for the periodic solution in terms of Jacobi elliptic functions. Here we investigate how these features manifest themselves for the emergent soliton solution. At first we solve the rotated Cauchy problem by implementing the profiles directly from the exact solution (4.3)

$$u(x, 0) = a\operatorname{sech}^2\left(\frac{a^{3/2}\sigma x}{6\sqrt{3}}\right), \quad u_t(x, 0) = \frac{a^{3/2}\sigma}{\sqrt{3}}\tanh\left(\frac{a^{3/2}\sigma x}{6\sqrt{3}}\right)\operatorname{sech}^2\left(\frac{a^{3/2}\sigma x}{6\sqrt{3}}\right),$$

$$u_{tt}(x, 0) = \frac{1}{6}a^2\sigma^2\left[\cosh\left(\frac{a^{3/2}\sigma x}{3\sqrt{3}}\right) - 2\right]\operatorname{sech}^4\left(\frac{a^{3/2}\sigma x}{6\sqrt{3}}\right), \qquad \lim_{|x|\to\infty} u(x, t) = 0. \tag{4.4}$$

Since the one-soliton solutions have finite compact support, the latter boundary value can be implemented numerically to a very high precision simply by taking the finite values of the interval in x to be very large. Thus, unlike as for periodic solutions of elliptic type, for the one-soliton solution the initial boundary value problem becomes a genuine Cauchy problem even when tackled numerically.

As seen in figure 5, for times up to around $t = 4$ the numerical solution smoothly follows the exact solution, but after that a visible singularity starts to develop at the origin in form of an ever growing oscillation which tends to infinity at $t \approx 6.34$. We notice that the oscillations are standing waves that do not make contributions to any of the charges, which for the values used in figure 5 are exactly identical to those obtained from the single soliton solution, i.e. $\mathcal{Q}_1 = 3.26599$, $\mathcal{Q}_2 = 2.17732$, $\mathcal{Q}_3 = 1.74186$ and $\mathcal{Q}_4 = 1.49302$.
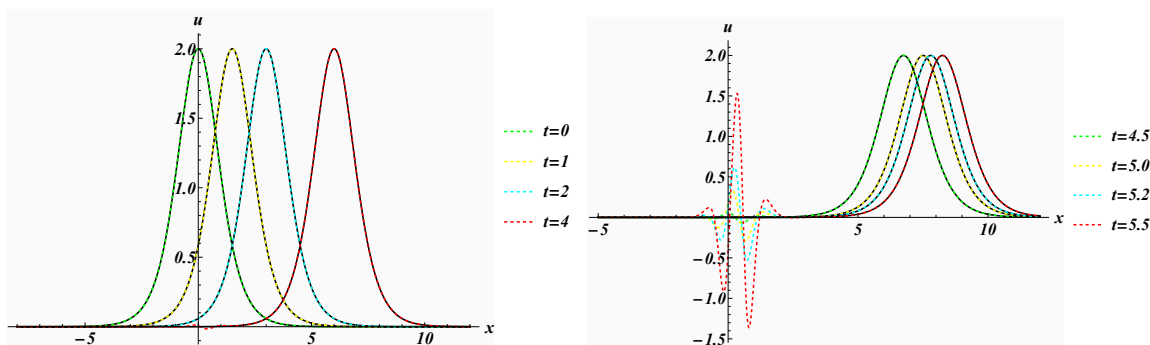
Figure 5. Evolution of the exact soliton solution (4.3) (solid black) versus the numerical solution (coloured dashed) of the rotated Cauchy problem for the KdV system with initial profiles (4.4) for $\sigma = 3$, $a = 2$ together with an emergent chargeless standing wave at the origin.

Next we solve the rotated Cauchy problem (4.1) for some more generic initial profile, here taken to be a Gaussian as in the previous section. We may then employ the same arguments as for the original unrotated case outlined in section 2 and predict the amplitudes of the emerging solitons. It turns out that for the solution (4.3) the values for the charges $\mathcal{Q}_\ell$ are exactly the same as those computed in (3.6), so that the general expressions for the bounds in (3.9) remain the same. However, the charges $\mathcal{Q}_\ell^{(I)}$ for the initial Gaussian profile are different in this case. We find $\mathcal{Q}_1^{(I)} = \sqrt{\pi/2^3}$, $\mathcal{Q}_2^{(I)} = \sqrt{\pi/3^3}$, $\mathcal{Q}_3^{(I)} = \sqrt{\pi/4^3}$, $\mathcal{Q}_4^{(I)} = \sqrt{\pi/5^3}$. Using the same argument as previously, we find that the two-soliton region (3.9) is now confined to the interval $\sigma_c < 2\sigma_c$ with $\sigma_c = 16 \times 6^{1/4}/\sqrt{\pi} \approx 14.1281$. In figure 6 we display the numerical solutions for the real square root amplitudes of the rotated version of the charge conservation equation (2.3).

Using the requirement that $\sqrt{a_i} \in \mathbb{R}^+$ for $i = 1, \dots, N$, we observe from figure 6 that only in the two soliton region a consistent solution may be found and no N-soliton solutions with $N > 2$ can be formed. For instance, considering the solution for $\ell = 1, 2, 3$ we observe that in the region $\sigma \lessapprox 39.85$ always one of the solutions is negative, whereas for $\sigma \gtrapprox 39.85$ only one of the solutions is real. Hence, no consistent three-soliton solution can be found. Indeed, this feature is confirmed by our numerical solutions shown in figure 7, for the initial profile $u(x,0) = e^{-x^2}$, $u_t(x,0) = u_{tt}(x,0) = 0$ and vanishing asymptotic conditions in x.

At the same time these predictions combine with the emerging of a singularity. For values of σ in the nonsoliton region $\sigma < \sigma_c$ we observe the emergence of a "defected" one-soliton and a single peakon that evolves into a single peak singularity. In contrast, for the larger values of σ in the two-soliton region $\sigma_c < \sigma < 2\sigma_c$, as predicted by (3.9), we see that the wave indeed starts to morphe into a two one-soliton structure, but before they are fully developed, the singularity in time has already occurred. We have verified that while the profiles evolve, the charges are conserved remaining $\mathcal{Q}_1 = 0.627$, $\mathcal{Q}_2 = 0.341$, $\mathcal{Q}_3 = 0.222$, $\mathcal{Q}_4 = 0.159$ in both cases. For various values of $\sigma > 2\sigma_c$ we have also verified that no N-soliton, not even in some indicated infant stage, begins to emerge. This agrees precisely with our predictions resulting from the charge conservation equations.
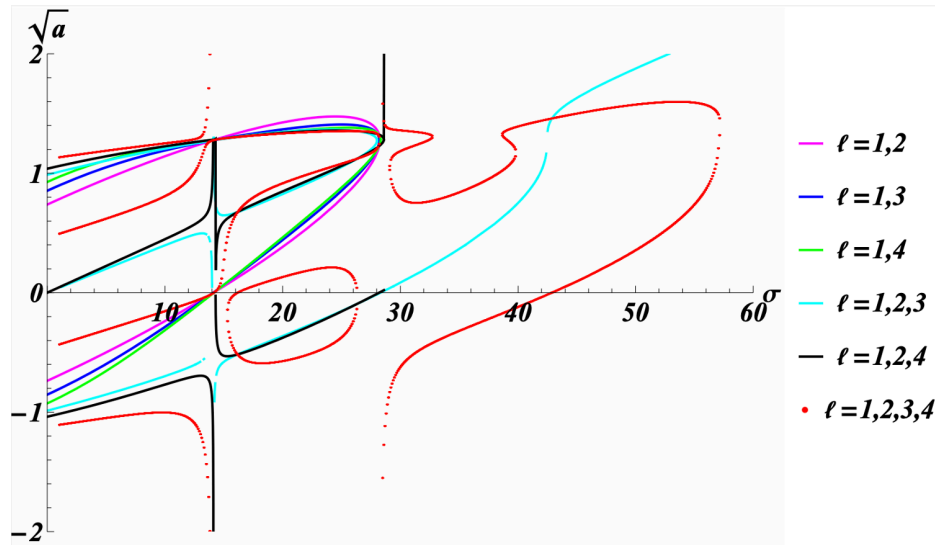
Figure 6. Predicted real square root amplitudes from different combinations of the rotated version of the charge conservation equation (2.3) with Gaussian initial profile in the HDT version of the mKdV-equation.
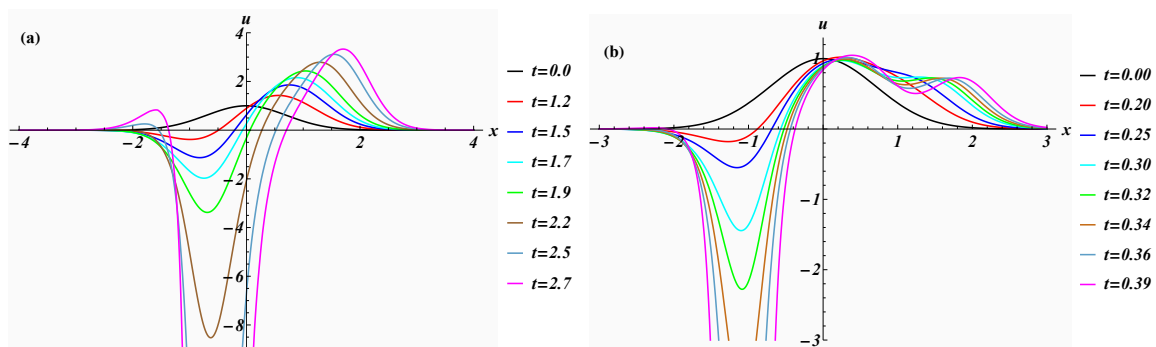
Figure 7. Evolution of a Gaussian, vanishing first and second order time-derivative initial profile for the rotated Cauchy problem of the KdV equation with $\sigma = 2$ in the nonsoliton region, panel (a) and $\sigma = 27$ in the two-soliton region, panel (b).

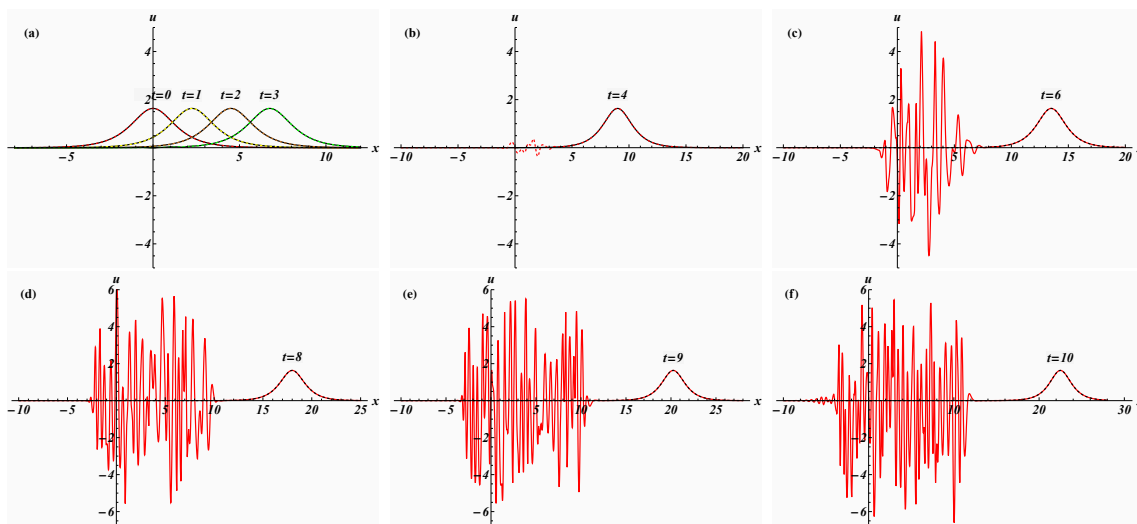### 4.2 Emergent solitons in the HTDT version of the modified KdV system

For the case $n = 4$ in (4.1) we find the exact one-soliton solution

$$u(x,t) = a \operatorname{sech}\left[\frac{a^3\sigma}{6\sqrt{6}}\left(x - \frac{6}{a^2}t\right)\right]. \tag{4.5}$$

At first we track this exact solution with the initial profiles directly corresponding to (4.5)

$$u(x,0) = a \operatorname{sech}\left(\frac{a^3\sigma}{6\sqrt{6}}x\right), \qquad u_t(x,0) = \frac{a^2\sigma}{\sqrt{6}}\tanh\left(\frac{a^3\sigma x}{6\sqrt{6}}\right)\operatorname{sech}\left(\frac{a^3\sigma x}{6\sqrt{6}}\right), \tag{4.6}$$

$$u_{tt}(x,0) = \frac{a^3\sigma^2}{12}\left[\cosh\left(\frac{a^3\sigma x}{3\sqrt{6}}\right) - 3\right]\operatorname{sech}^3\left(\frac{a^3\sigma x}{6\sqrt{6}}\right), \qquad \lim_{|x|\to\infty} u(x,t) = 0.$$

Figure 8. Evolution of the exact soliton solution (4.5) (dashed black) versus the numerical solution (red solid) of the rotated Cauchy problem for the modified KdV system with initial profiles (4.6) with an emergent standing wave at the origin for $\sigma = 3$ and $a = 2\sqrt{2/3}$.

Unlike as in the HTD version of the KdV systems we can track this exact one-soliton solution quite precisely to arbitrary large time as depicted in figure 8.

We also observe that similarly as for the HTD version of the KdV system oscillations start to emerge near the origin, but crucially in this case they remain finite in amplitude.

Next we probe what happens when we send in an arbitrary initial profile. The charges corresponding to the solution (4.5) are the same as in the unrotated case (3.22). However, the charges corresponding to the Gaussian initial profile are different

$$\mathcal{Q}_n^{(I)} = \sqrt{\frac{\pi}{8\,(n+1)^3}}, \qquad n = 1, 2, \ldots \tag{4.7}$$

so that the predictions for the amplitudes from the conservation laws will also vary. Our predictions are depicted in figure 9.

Unlike as in the HTD version of KdV, now negative amplitudes in the solution (4.5) are permitted, since $a \to -a$ leads to $u \to -u$, which is also a solution of (4.1) for n even. Thus we see that for $\sigma \lesssim 39.85$ all of the calculated possibilities for N-soliton solutions are actually realised, i.e., $N = 2, 3, 4, 5$. We conjecture that this will hold also beyond the cases we have computed for all $N > 5$. In the region for $\sigma \gtrsim 39.85$ only solutions for $N > 4$ are acquired.

The overall effect on the evolution of the initial profile is that the localised wave tries to decay into N-soliton soltions with larger and large N as time evolves. We conjecture that this feature is responsible for the oscillatory behaviour as seen in figure 10. In the positive x-region we can identify the various N-soliton solutions that can be realised at different times and notice further that for larger values of σ the larger N-soliton solutions are settled into much quicker. At the same time the overall behaviour remains *benign* (or *metastable* [48]), in the sense that all the solutions for the amplitudes predicted from different conservation laws are finite.
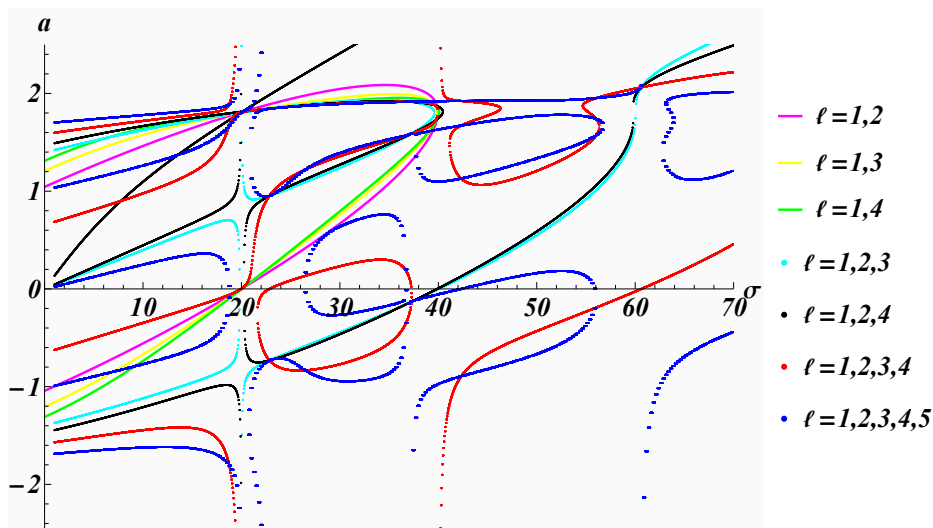
Figure 9. Predicted real amplitudes from different combinations of the rotated version of the charge conservation equation (2.3) with Gaussian initial profile in the HDT version of the mKdV-equation.
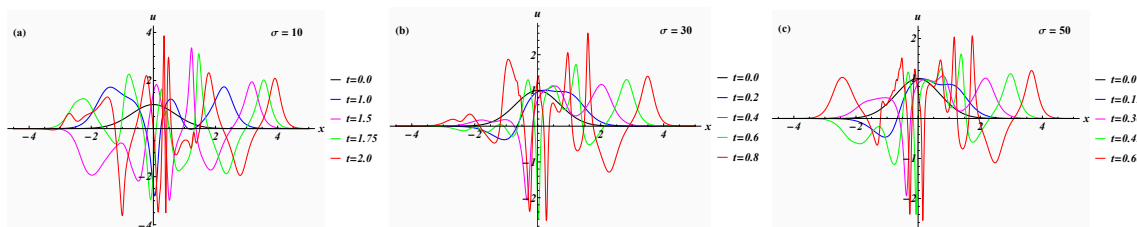
Figure 10. Evolution of a Gaussian, vanishing first and second order time-derivative initial profile for the HTD version of the modified KdV equation in different characteristic regions.

4.3 Solitary waves in nonintegrable HTD mKdV systems

Finally, we investigate the HTD systems with $n > 4$, which are not integrable. The latter means that we do not expect soliton solutions to appear, but also that all the restrictions imposed by the conservation laws are absent. Our explicit computations show that all models with n odd and $n > 4$ behave for all σ qualitatively in the same manner as the $n = 3$ theory in the nonsoliton regime. For n even and $n > 4$ we observe a similar, but more random behaviour as in the $n = 4$ model.

5 Conclusions

In the first part we have revisited the problem of how an initial localised profile evolves when propagated by means of nonlinear modified KdV systems. Exploiting the integrability of some of these systems, we used various combinations of conservation laws to predict the number of solitons into which the profile will be permitted to settle into, as well as their respective amplitudes. By refining the previously carried out analysis, we found that an initial profile will always decay into the maximal number of N-solitons that is allowed by the conservation laws. We conjecture that this is a general feature. For the nonintegrable versions of these theories we found that in the $n = 5$ case the features of the nonsoliton regime

of the integrable systems are still present. In that case a solitary wave moving at constant speed emerged together with an oscillatory tail at negative x. No decay into multi-solitons was observed. For all other cases with we found that the profile will always evolve into the oscillatory tail that will eventually distribute the charge into all modes.

When adapting the analysis to the higher time-derivative versions of these theories, we derived that the only allowed breakup, by integrability, of the initial profile is into a two-soliton solution for the $n = 3$ case. This feature then combines with the previously observed property that the classical solutions of these theories will develop instabilities [40–42], as is to be expected in HTDT. For the exact solutions of the HTD-KdV system the singularities manifest themselves as chargeless standing waves at the origin, whose amplitudes grow to infinity as time evolves. Instead, in the HTD-mKdV system we found that the profile is allowed to settle into any of the N-soliton solutions, which gives rise to the oscillations spreading out from the origin. As the solutions for all of the predicted amplitudes is finite, these oscillations do not grow to infinity. For the nonintegrable theories with n odd we found the same behaviour as for the $n = 3$ theory in the nonsoliton region. For the cases with n even we found that the disturbance settles into a more random set of oscillations. We noticed that the soliton/solitary waves in the HTDT are usually slower when compared to their first order time-derivative counterparts. The spreading speed of the oscillations is faster in all observed cases so that the solitary wave structures were always found to be absorbed by the oscillations spreading out.

There are some obvious open questions. Here we have always taken a simple Gaussian as initial profile $u(x, 0) = e^{-x^2}$, and have set the independent profiles for the first and second order time-derivative to zero. We found that changing the time derivative profiles does not change the overall characteristic behaviour, but a more systematic analysis, using different options for these profiles, would be interesting to obtain. It would be especially insightful to find out whether it is possible to prolong the lifetime of the soliton/solitary wave structures to such an extend that they can fully develop before being absorbed by the oscillations. Evidently, it would be interesting to develop analytical arguments that predict the speed of the spread of the oscillation study and to study the observed effect in other types of integrable models.

Acknowledgments

References

[1] N.J. Zabusky and M.D. Kruskal, *Interaction of "solitons" in a collisionless plasma and the recurrence of initial states*, *Phys. Rev. Lett.* **15** (1965) 240 [InSPIRE].

[2] E. Fermi, P. Pasta, S. Ulam and M. Tsingou, *Studies of the nonlinear problems*, Technical report, Los Alamos National Lab. (LANL), Los Alamos, NM, U.S.A., (1955).

[3] G.P. Berman and F.M. Izrailev, *The Fermi-Pasta-Ulam problem: Fifty years of progress*, *Chaos* **15** (2005) 015104 [nlin/0411062].

[4] Y.A. Berezin and V.I. Karpman, *Nonlinear evolution of disturbances in plasmas and other dispersive media*, *Sov. Phys. JETP* **24** (1967) 1049.

[5] A. Jeffrey and T. Kakutani, *Weak nonlinear dispersive waves: a discussion centered around the Korteweg-de Vries equation*, *SIAM Rev.* **14** (1972) 582.

[6] A. Pais and G.E. Uhlenbeck, *On field theories with non-localized action*, *Phys. Rev.* **79** (1950) 145 [INSPIRE].

[7] K.S. Stelle, *Renormalization of higher-derivative quantum gravity*, *Phys. Rev. D* **16** (1977) 953 [INSPIRE].

[8] A.A. Starobinsky, *A new type of isotropic cosmological models without singularity*, *Phys. Lett. B* **91** (1980) 99 [INSPIRE].

[9] S.L. Adler, *Einstein gravity as a symmetry-breaking effect in quantum field theory*, *Rev. Mod. Phys.* **54** (1982) 729 [*Erratum ibid.* **55** (1983) 837] [INSPIRE].

[10] A.V. Smilga, *Spontaneous generation of the Newton constant in the renormalizable gravity theory*, arXiv:1406.5613 [INSPIRE].

[11] L. Modesto and I.L. Shapiro, *Superrenormalizable quantum gravity with complex ghosts*, *Phys. Lett. B* **755** (2016) 279 [arXiv:1512.07600] [INSPIRE].

[12] T.-J. Chen, M. Fasiello, E.A. Lim and A.J. Tolley, *Higher derivative theories with constraints: Exorcising Ostrogradski's Ghost*, *JCAP* **02** (2013) 042 [arXiv:1209.0583] [INSPIRE].

[13] A. Salvio and A. Strumia, *Quantum mechanics of 4-derivative theories*, *Eur. Phys. J. C* **76** (2016) 227 [arXiv:1512.01237] [INSPIRE].

[14] D. Anselmi, *Fakeons and Lee-Wick models*, *JHEP* **02** (2018) 141 [arXiv:1801.00915] [INSPIRE].

[15] C.M. Bender and P.D. Mannheim, *No-ghost theorem for the fourth-order derivative Pais-Uhlenbeck oscillator model*, *Phys. Rev. Lett.* **100** (2008) 110402 [arXiv:0706.0207] [INSPIRE].

[16] M. Raidal and H. Veermäe, *On the quantisation of complex higher derivative theories and avoiding the Ostrogradsky ghost*, *Nucl. Phys. B* **916** (2017) 607 [arXiv:1611.03498] [INSPIRE].

[17] S.W. Hawking and T. Hertog, *Living with ghosts*, *Phys. Rev. D* **65** (2002) 103515 [hep-th/0107088] [INSPIRE].

[18] T. Biswas, T. Koivisto and A. Mazumdar, *Towards a resolution of the cosmological singularity in non-local higher derivative theories of gravity*, *JCAP* **11** (2010) 008 [arXiv:1005.0590] [INSPIRE].

[19] A. Salvio, *Dimensional transmutation in gravity and cosmology*, *Int. J. Mod. Phys. A* **36** (2021) 2130006 [arXiv:2012.11608] [INSPIRE].

[20] A. Salvio, *Quasi-conformal models and the early universe*, *Eur. Phys. J. C* **79** (2019) 750 [arXiv:1907.00983] [INSPIRE].

[21] A. Salvio, *A non-perturbative and background-independent formulation of quadratic gravity*, *JCAP* **07** (2024) 092 [arXiv:2404.08034] [INSPIRE].

[22] H.A. Weldon, *Finite-temperature retarded and advanced fields*, *Nucl. Phys. B* **534** (1998) 467 [hep-ph/9803478] [INSPIRE].

[23] S. Mignemi and D.L. Wiltshire, *Black holes in higher-derivative gravity theories*, *Phys. Rev. D* **46** (1992) 1475 [`hep-th/9202031`] [INSPIRE].

[24] V.O. Rivelles, *Triviality of higher derivative theories*, *Phys. Lett. B* **577** (2003) 137 [`hep-th/0304073`] [INSPIRE].

[25] D.S. Kaparulin, S.L. Lyakhovich and A.A. Sharapov, *BRST analysis of general mechanical systems*, *J. Geom. Phys.* **74** (2013) 164 [`arXiv:1207.0594`] [INSPIRE].

[26] M.S. Plyushchay, *Massless point particle with rigidity*, *Mod. Phys. Lett. A* **4** (1989) 837 [INSPIRE].

[27] M.S. Plyushchay, *Massless particle with rigidity as a model for the description of bosons and fermions*, *Phys. Lett. B* **243** (1990) 383 [INSPIRE].

[28] M. Dine and N. Seiberg, *Comments on higher derivative operators in some SUSY field theories*, *Phys. Lett. B* **409** (1997) 239 [`hep-th/9705057`] [INSPIRE].

[29] A. Smilga, *Ultraviolet divergences in non-renormalizable supersymmetric theories*, *Phys. Part. Nucl. Lett.* **14** (2017) 245 [`arXiv:1603.06811`] [INSPIRE].

[30] M. Pavšič, *Stable Self-Interacting Pais-Uhlenbeck Oscillator*, *Mod. Phys. Lett. A* **28** (2013) 1350165 [`arXiv:1302.5257`] [INSPIRE].

[31] D.S. Kaparulin, S.L. Lyakhovich and A.A. Sharapov, *Classical and quantum stability of higher-derivative dynamics*, *Eur. Phys. J. C* **74** (2014) 3072 [`arXiv:1407.8481`] [INSPIRE].

[32] M. Avendaño-Camacho, J.A. Vallejo and Y. Vorobiev, *A perturbation theory approach to the stability of the Pais-Uhlenbeck oscillator*, *J. Math. Phys.* **58** (2017) 093501 [`arXiv:1703.08929`] [INSPIRE].

[33] N. Boulanger, F. Buisseret, F. Dierick and O. White, *Higher-derivative harmonic oscillators: stability of classical dynamics and adiabatic invariants*, *Eur. Phys. J. C* **79** (2019) 60 [`arXiv:1811.07733`] [INSPIRE].

[34] C. Deffayet, S. Mukohyama and A. Vikman, *Ghosts without runaway instabilities*, *Phys. Rev. Lett.* **128** (2022) 041301 [`arXiv:2108.06294`] [INSPIRE].

[35] C. Deffayet, A. Held, S. Mukohyama and A. Vikman, *Global and local stability for ghosts coupled to positive energy degrees of freedom*, *JCAP* **11** (2023) 031 [`arXiv:2305.09631`] [INSPIRE].

[36] A.V. Smilga, *On exactly solvable ghost-ridden systems*, *Phys. Lett. A* **389** (2021) 127104 [`arXiv:2008.12966`] [INSPIRE].

[37] V.G. Samoilenko and N.N. Pritula and U.S. Suyarov, *The complete integrability analysis of the inverse Korteweg-de Vries equation*, *Ukr. Math. J.* **43** (1991) 1157.

[38] A. Fring and B. Turner, *Higher derivative Hamiltonians with benign ghosts from affine Toda lattices*, *J. Phys. A* **56** (2023) 295203 [`arXiv:2301.11317`] [INSPIRE].

[39] A. Fring and B. Turner, *Integrable scattering theory with higher derivative Hamiltonians*, *Eur. Phys. J. Plus* **138** (2023) 1136 [`arXiv:2307.15210`] [INSPIRE].

[40] A. Fring, T. Taira and B. Turner, *Higher Time-Derivative Theories from Space-Time Interchanged Integrable Field Theories*, *Universe* **10** (2024) 198 [`arXiv:2403.11949`] [INSPIRE].

[41] T. Damour and A. Smilga, *Dynamical systems with benign ghosts*, *Phys. Rev. D* **105** (2022) 045018 [`arXiv:2110.11175`] [INSPIRE].

[42] A. Smilga, *Modified Korteweg-de Vries equation as a system with benign ghosts*, *Acta Polytech.* **62** (2022) 190 [`arXiv:2112.14120`] [INSPIRE].

[43] G.B. Whitham, *Non-linear dispersive waves*, *Proc. R. Soc. Lond. A. Math. and Phys. Sci.* **283** (1965) 238.

[44] R.M. Miura, *Korteweg-de Vries equation and generalizations. I. A remarkable explicit nonlinear transformation*, *J. Math. Phys.* **9** (1968) 1202.

[45] R.M. Miura, C.S. Gardner and M.D. Kruskal, *Korteweg-de Vries equation and generalizations. II. Existence of conservation laws and constants of motion*, *J. Math. Phys.* **9** (1968) 1204.

[46] Y. Nutku, *Hamiltonian formulation of the KdV equation*, *J. Math. Phys.* **25** (1984) 2007 [INSPIRE].

[47] V.I. Karpman, *An asymptotic solution of the Korteweg-de Vries equation*, *Phys. Lett. A* **25** (1967) 708.

[48] A. Salvio, *Metastability in quadratic gravity*, *Phys. Rev. D* **99** (2019) 103507 [arXiv:1902.09557] [INSPIRE].